

Identification of two-phase flow regimes based on support vector machine and electrical capacitance tomography

H X Wang^{1,3} and L F Zhang^{1,2}

¹ School of Electrical Engineering and Automation, Tianjin University, Tianjin 300072, People's Republic of China

² School of Control Science and Engineering, North China Electric Power University, Baoding 071003, People's Republic of China

E-mail: hxwang@tju.edu.cn

Received 20 January 2009, in final form 11 March 2009

Published 18 September 2009

Online at stacks.iop.org/MST/20/114007

Abstract

It is important to identify two-phase flow regimes for the accuracy measurement of other flow parameters. Electrical capacitance tomography (ECT) is often used to identify two-phase/multi-phase flow regimes. The support vector machine (SVM) is a machine-learning algorithm based on the statistical learning theory, which has desirable classification ability with fewer training samples, and can be used for flow regime identification. The capacitance measurement data obtained from an ECT system contain flow regime information. The principal component analysis method has been used to reduce the dimension of the capacitance measurements. Simulation was carried out using the SVM method. The results show its feasibility. Static and dynamic experiments were also done for typical flow regimes, and the results indicate that this method is fast in speed and can identify these flow regimes correctly

Keywords: two-phase flow, support vector machine, electrical capacitance tomography, flow regime identification

(Some figures in this article are in colour only in the electronic version)

1. Introduction

Two-phase flows exist widely in the petroleum, chemical and power industry. The distribution state of each phase in a two-phase flow is called a flow regime. It is important to know flow regimes for the analysis and measurement of two-phase flows [1–3]. However, all currently available methods of measuring the flow rate of two-component mixtures in industrial pipelines commonly take the average of the flow rate over the pipe cross-section, without flow regime information. Therefore, they are unsuitable for accurate measurement where the component distributions are spatially or temporally varying.

Process tomography is a technique of flow imaging. There are many kinds of process tomography techniques,

such as electrical capacitance tomography (ECT), electrical impedance tomography (EIT) and optical tomography [4, 5].

The ECT technique has been extensively investigated during the past few decades as a visualization technique for measurement and imaging of two-phase flows in real time in [6, 7]. This technique involves a number of capacitive electrodes mounted circumferentially around a flow pipe and relies on the changes in capacitance between the electrodes owing to the change in the permittivity of flow components, as shown in figure 1.

Capacitances are measured between different electrode pairs, and the measurements obtained are used to reconstruct a cross-sectional distribution of flow components. For a 12-electrode system, the number of independent capacitance measurements is 66. ECT is composed of a forward problem and inverse problem. The forward problem is to determine

³ Author to whom any correspondence should be addressed.

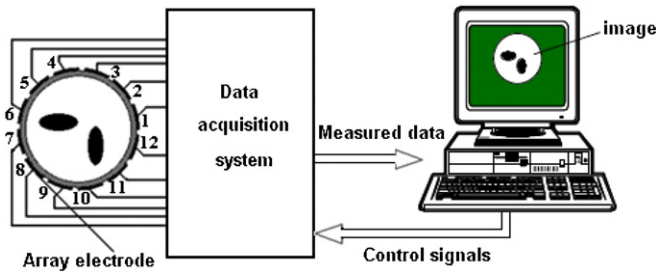


Figure 1. Typical ECT system with a 12-electrode sensor.

capacitance measurements. The inverse problem is also called image reconstruction [8, 9].

There are two methods for identification of flow regimes based on ECT. One method is based on image reconstruction [10–16]. The other is based on the sensor outputs of ECT [17–19]. The advantage of the first method is that the flow regime can be visualized. The disadvantages lie in its speed and quality for image reconstruction. For the latter, there is no need to reconstruct images and hence it saves time. In the meantime, a reconstructed image in itself can seldom be directly used for control purposes. The second method is more suitable for online flow regime identification and control than the first method.

As we can see, neural networks are often used to give the identification result of flow regimes after training for the second method. Hundreds of training samples are needed for network training to obtain a good prediction accuracy and generalization ability. The support vector machine (SVM) is a machine-learning algorithm based on the statistical learning theory (SLT), which has desirable classification ability with fewer training samples, and can be used for flow regime identification.

This paper investigates the identification of flow regimes for oil–gas two-phase flows using the SVM and the outputs of the ECT sensor without image reconstruction, as the capacitance measurements (the inputs of the SVM) contain flow regime information. The dimension of the inputs is reduced using the principal component analysis (PCA) method, and the SVM method is then used to identify the flow regimes.

2. Classification mechanism of the SVM

2.1. Basic concept of the SVM classifier

The SVM technique was proposed by Vapnik [20]. It is a new learning system based on recent advances in the statistical learning theory. The SVM delivers state-of-the-art performance in many real-world predictive data mining applications such as text categorization, medical and biological information analysis [21, 22]. Theoretically, the main reason for the superior performance is that the SVM embodies the structural risk minimization (SRM) principle to minimize an upper bound on the expected risk. The SVM has great ability to avoid over-fitting and thus can be generalized to predict new data that are not included in the training dataset.

Geometrically, an SVM modeling algorithm builds a separating hyper-plane with the maximal margin. For

classification, the SVM operates by finding a hyper-plane in the space of possible inputs, i.e. the original input feature space or after-kernel-transformed feature space. This hyper-plane attempts to separate the positive samples from the negative samples. The separation is chosen so that the distance from the hyper-plane is nearest to the positive and negative samples. Intuitively, this makes the classification correct for testing data that are near, but not identical to, the training data.

Given a training set of the linear separation pairs (x_i, y_i) , $i = 1, 2, \dots, m$, where $x_i \in R^n$ and class label is $y_i \in \{+1, -1\}$, the SVM finds an optimal separating hyper-plane with the maximum margin by solving the following optimization problem:

$$\begin{aligned} & \text{Min}_{w,b} w^T w / 2 \\ & \text{Subject to } y_i ((w \cdot x_i) + b) - 1 \geq 0. \end{aligned} \quad (1)$$

To solve this quadratic optimization problem, the saddle point of the Lagrange function must be found:

$$L_p(w, b, \alpha) = \frac{1}{2} w^T w - \sum_{i=1}^m (\alpha_i y_i ((w \cdot x_i) + b) - 1), \quad (2)$$

where α_i denotes the Lagrange multipliers.

It is necessary to search for an optimal saddle point because L_p must be minimized with respect to the primal variables w and b and maximized with respect to the non-negative variable α_i . By differentiating with respect to w and b , equation (2) is transformed to the dual Lagrangian $L_D(\alpha)$:

$$\begin{aligned} & \text{Max}_{\alpha} L_D(\alpha) = \sum_{i=1}^m \alpha_i - \frac{1}{2} \sum_{i,j=1}^m \alpha_i \alpha_j y_i y_j (x_i \cdot x_j) \\ & \text{Subject to } \alpha_i \geq 0, i = 1, 2, \dots, m \text{ and } \sum_{i=1}^m \alpha_i y_i = 0. \end{aligned} \quad (3)$$

To find the optimal hyper-plane, a dual Lagrangian $L_D(\alpha)$ must be maximized with respect to non-negative α_i . The solution α_i for the dual optimization problem determines the parameters w^* and b^* of the optimal hyper-plane. Thus, the optimal hyper-plane decision function $f(x) = \text{sgn}((w^* \cdot x) + b^*)$ can be written as

$$f(x) = \text{sgn} \left(\sum_{i=1}^m y_i \alpha_i^* (x_i \cdot x) + b^* \right). \quad (4)$$

In a typical classification task, only a small subset of the Lagrange multipliers α_i usually tends to be greater than zero. Geometrically, these vectors are the closest to the optimal hyper-plane. The respective training vectors having non-zero α_i are called support vectors, as the optimal decision hyper-plane $f(x, \alpha^*, b^*)$ depends on them exclusively.

The nonlinear SVM maps the training samples from the mapping function ϕ . The kernel function $k(x_i, x_j)$ defines an inner product as $k(x_i, x_j) = \phi(x_i) \cdot \phi(x_j)$.

Following the steps described above, a decision function is obtained:

$$\begin{aligned} f(x) &= \text{sgn} \left(\sum_{i=1}^m y_i \alpha_i^* (x_i \cdot x) + b^* \right) \\ &= \text{sgn} \left(\sum_{i=1}^m y_i \alpha_i^* (k(x_i, x)) + b^* \right). \end{aligned} \quad (5)$$

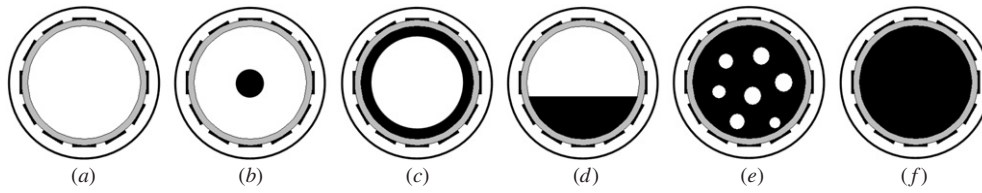


Figure 2. Flow regimes to be identified: (a) empty-pipe flow, (b) core flow, (c) annular flow, (d) stratified flow, (e) bubbly flow and (f) full-pipe flow.

The kernel function is the radial basis function (RBF), which is defined by

$$k(x_i, x_j) = \exp(-\gamma \|x_i - x_j\|^2). \quad (6)$$

2.2. Multi-class identification algorithm of the SVM

Two methods are commonly used to construct an SVM multi-class classifier. One is the 1-against-rest (1-a-r), which was presented by Vapnik [20]. In this method, one SVM classifier separates one class from the other classes. The number of SVM classifiers needed is equal to that of the classes. The other method is 1-against-1 (1-a-1) presented by Krebel. It constructs all the possible two-class classifiers. Every class is trained on the two-class training sets. If there are P classes, $P(P - 1)/2$ classifiers are needed. For the 1-against-1 algorithm, a new learning structure called a decision directed acyclic graph (DDAG) was proposed by Platt [23]. It contains $P(P - 1)/2$ nodes. The node on the top layer is called the root node. The i th layer contains i nodes and the i th node on the j th layer points to the i th and $i+1$ th nodes on the $j+1$ th layer.

3. Basic properties of PCA

Principal component analysis (PCA) is a data-driven technique used to explain the variance–covariance structure of the dataset through a set of linear combinations of the original variables. The PCA transform has been widely used in statistical data analysis and pattern recognition [24, 25].

Given an observed n_s -dimensional vector \mathbf{x} , the goal of PCA is to reduce the dimensionality of \mathbf{X} . This is realized by finding n_r principal axes $\mathbf{p}_i, i = 1, 2, \dots, n_r$, onto which the variance retained under projection is maximal. These axes, denoted as principal directions, are given by the eigenvectors associated with the n_s largest eigenvalues $\lambda_i, i = 1, 2, \dots, n_s$, of the covariance matrix [26]:

$$\sum = E[(\mathbf{x} - \mu)(\mathbf{x} - \mu)^T],$$

where $E[\cdot]$ is the expectation and μ is the mean of \mathbf{x} .

n_r is determined by the accumulation contribution ratio of the n_r largest eigenvalues, which is defined as

$$Q(n_r) = \frac{\sum_{i=1}^{n_r} \lambda_i}{\sum_{i=1}^{n_s} \lambda_i},$$

where $Q(n_r)$ is commonly considered to be larger than 85%, and hence n_r can be determined.

If the principal directions are collected in a matrix $\mathbf{P} = [\mathbf{p}_1 \cdots \mathbf{p}_{n_r}]$, then $\mathbf{z} = \mathbf{P}^T(\mathbf{x} - \mu)$ is a reduced n_r -dimensional representation of the observed vector \mathbf{x} . Among

all linear techniques, PCA provides the optimal reconstruction $\hat{\mathbf{x}} = \mu + \mathbf{Pz}$ of \mathbf{x} in terms of the quadratic reconstruction error $\|\mathbf{x} - \hat{\mathbf{x}}\|^2$.

One advantage of PCA is its ability to describe the data using a small group of underlying variables while preserving as much of the relevant information as possible in the dimensionality reduction process.

Using the PCA method, the dimension of the inputs (66 capacitance measurements) is reduced, which can increase the speed of the SVM algorithm.

4. Experiment

4.1. Flow regimes

In this paper, oil–gas two-phase flows are studied. The flow regimes to be identified are shown in figure 2 (oil in black and gas in white).

For image reconstruction, it is a common practice to use the normalized capacitance, which is defined by [9]

$$\lambda = \frac{C_m - C_l}{C_h - C_l}, \quad (7)$$

where C_m is the measured capacitance when objects are present in the sensor and C_l and C_h are the capacitance values when the sensor is completely filled with a low permittivity material and high permittivity material, respectively. The normalized capacitance measurement data corresponding to these six flow regimes are shown in figure 3.

4.2. Simulation

A DDAG for the identification of these six flow regimes (each denotes one class) in figure 2 is designed, as shown in figure 4.

The training sets were obtained by simulation using finite element software developed by the authors. The field was dissected as shown in figure 5. The sensing fields measured inside the pipe, pipe wall and the space between the pipe wall and screen were dissected into five, three and two layers, respectively.

(1) *Selection of core flow samples.* The first layer inside the pipe field was selected as the first core flow sample and the first and the second layers were then together selected as the second sample. According to this rule, four core flow samples can be obtained. Then, the field can be dissected into different layers. More core flow samples can be obtained. In this paper, 30 core flow samples were selected.

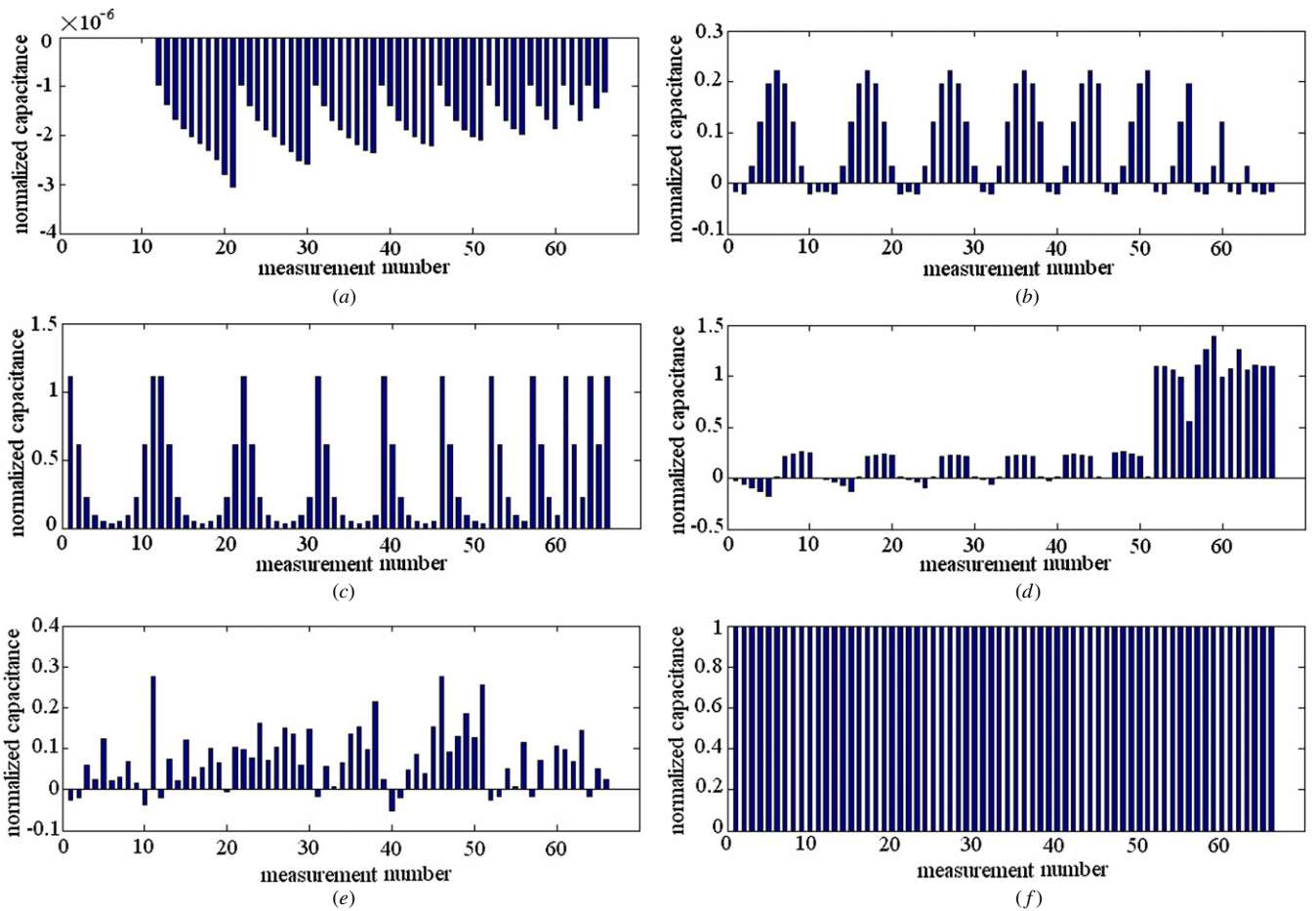


Figure 3. Normalized capacitance measurements: (a) empty-pipe flow, (b) core flow, (c) annular flow, (d) stratified flow, (e) bubbly flow and (f) full-pipe flow.

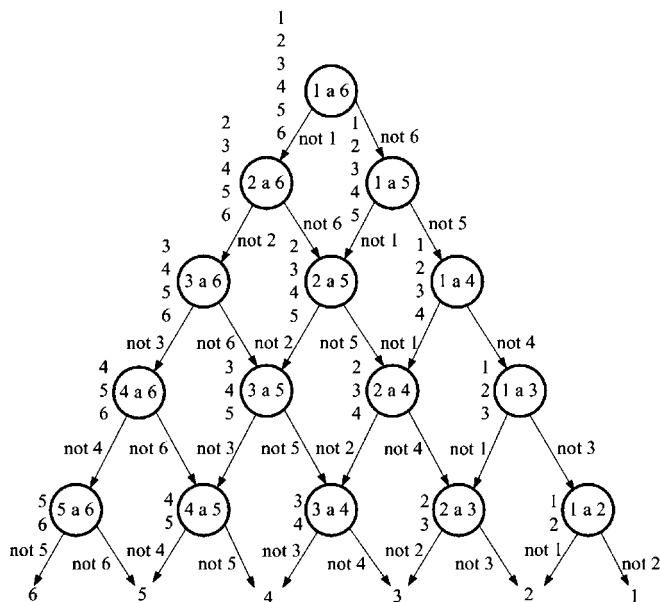


Figure 4. DDAG structure for six classes.

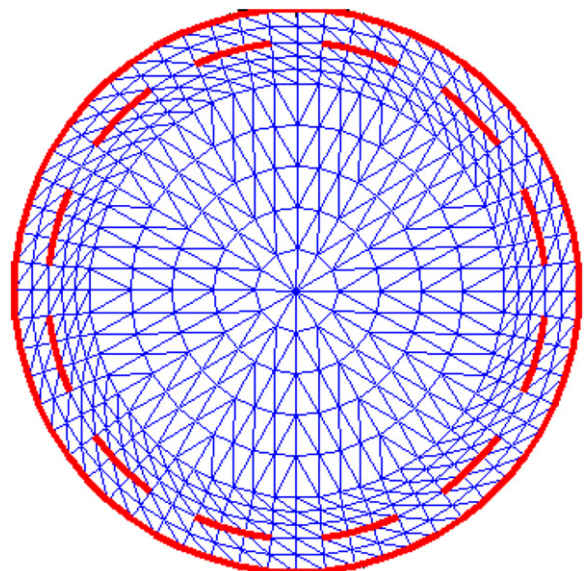


Figure 5. Mesh grid.

(2) *Selection of annular flow samples.* The fifth layer inside the pipe field was selected as the first annular flow sample

and the fourth and the fifth layers were then together selected as the second sample. According to this rule, four annular flow samples can be obtained. Then, the

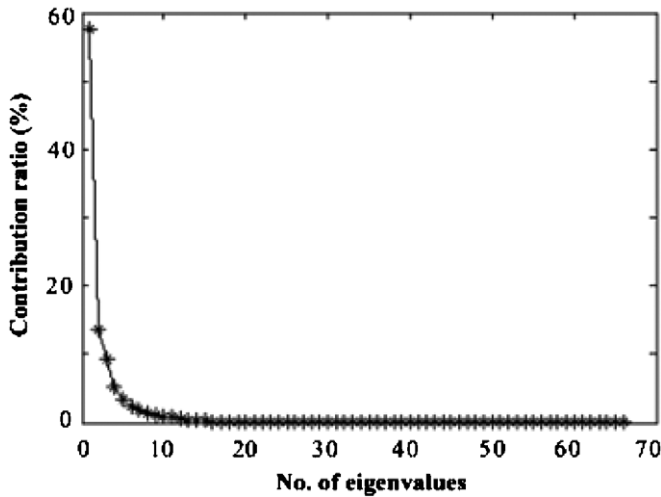


Figure 6. Contribution ratio of each eigenvalue.

field can be dissected into different layers. More annular flow samples can be obtained. In this paper, 30 annular flow samples were selected.

- (3) *Selection of stratified flow samples.* The pipe was divided into 11 sections along the vertical diameter, and ten stratified flow samples were obtained.
- (4) *Selection of bubbly flow samples.* 40 bubbly flow samples were selected by setting some elements to be bubbles. To improve the identification accuracy, homogeneous bubble distributions are simulated.
- (5) *Selection of empty-pipe and full-pipe flow samples.* There is only one empty-pipe or full-pipe flow sample. To simulate the real measurement noise, different noise, from 0.1 to 5%, was added to the capacitance values, and ten empty-pipe flow and ten full-pipe flow samples were obtained.

Table 1. Iterative values of γ .

No	γ	e	$\Delta\gamma = (e/n)\gamma$
1	1.2	7	0.084
2	1.284	5	0.0642
3	1.3482	5	0.0674
4	1.4156	4	0.0566
5	1.4722	2	0.0294
6	1.5016	1	0.0150
7	1.5166	1	0.0152
8	1.5318	0	0

130 samples were obtained. 100 groups were selected to be training sets and 30 groups were selected to be test sets. Using the PCA method, the contribution ratio of each eigenvalue is shown in figure 6.

14 principal components were selected, which greatly decrease the dimension of the inputs. The accumulation contribution ratio of the 14 eigenvalues is 99.02%.

The RBF kernel function was selected. Parameter γ will affect the classification results. A proper value of γ must be selected. In this paper, the iterative algorithm based on the number of sets, which were not classified correctly, was adopted to decide the value of γ . The first step is to train the network with a small initial value of γ , and then the incorrect classification number of the SVM method for the training sets is obtained:

$$e = \sum_{i,j=1,i \neq j}^m r_{ij}, \tag{8}$$

where m is the total classes and r_{ij} is the incorrect classification number of training sets which belong to the i th class but are identified as the j th class. Finally, the value of γ can be modified using

$$\gamma_{k+1} = \gamma_k + (e/n)\gamma_k, \tag{9}$$

where n is the number of training sets. If $e \neq 0$, the value of

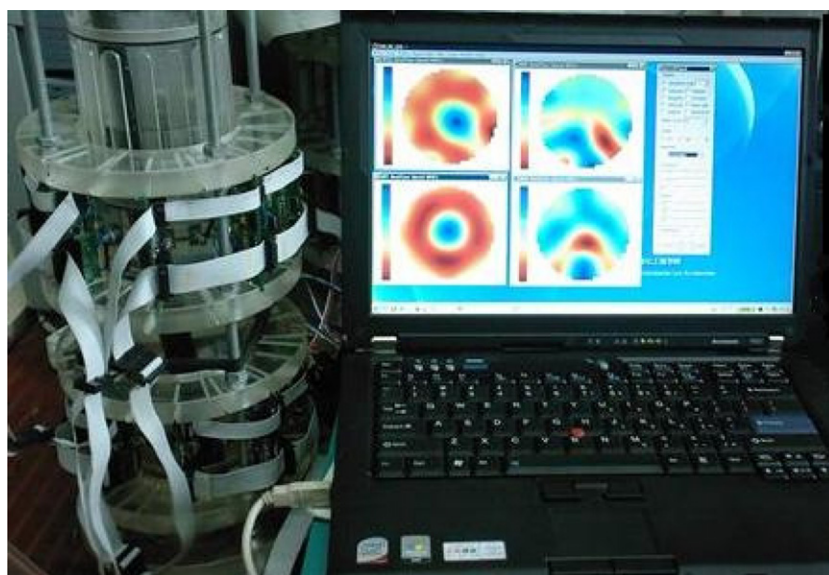


Figure 7. Twin-plane dual-modality electrical tomography (ECT/ERT) system.

Table 2. Identification results for simulation test data.

Flow regime	Empty-pipe	Core	Annular	Stratified	Bubbly	Full-pipe
Total	3	6	6	4	8	3
Correct	3	5	5	4	6	3
Identification rate	100%	83.3%	83.3%	100%	75%	100%

Table 3. System specifications.

	TJU_ET_III (ECT modality)	TJU_ET_III (ERT modality)
Electrode number	Twin-plane sensor, each with 8, 12, 16 electrodes	Twin-plane sensor, each with 8, 12, 16 electrodes
Property of interest	Permittivity	Conductivity
Excitation signal	ac-based sine wave voltage	ac-based sine wave current
Amplitude	0.5–18 V (pp), adjustable	1–20 mA (pp), adjustable
Frequency	1 kHz–1 MHz, adjustable	1 kHz–1 MHz, adjustable
Data acquisition rate	500 frame s ⁻¹	500 frame s ⁻¹
Algorithm	Linear back projection (LBP), Tikhonov, pre-iteration, etc	Linear back projection (LBP), Tikhonov, pre-iteration, etc
Online imaging speed	100 frame s ⁻¹ (pre-iteration algorithm)	100 frame s ⁻¹ (pre-iteration algorithm)
Image spatial resolution	5–8%	5–8%
Data transfer	USB 2.0	USB 2.0

γ must be calculated repeatedly until $e = 0$. The values of γ calculated according to this method are listed in table 1.

On a PC with a Pentium™ 4 2.0 GHz CPU and 512 M memory, the training time is 57 s. After training, the 30 groups' testing data were used to test the classification performance of the SVM method. The results are given in table 2 and the test time is 0.39 s. It can be seen that the empty-pipe, stratified and full-pipe flows can be identified correctly. For the core flow and annular flow, the correct identification rate is 83.3%. The reason for the incorrect identifications is because the area of the core flow or the annular flow sample is very close to that of the full-pipe flow. Because a bubbly flow can vary greatly, therefore the correct identification is only 75%. If more samples are selected for bubbly flows, a higher identification rate may be reached. Simulation indicates that the identification method based on the SVM and ECT is feasible. To verify the presented method, static and dynamic experiments were also carried out.

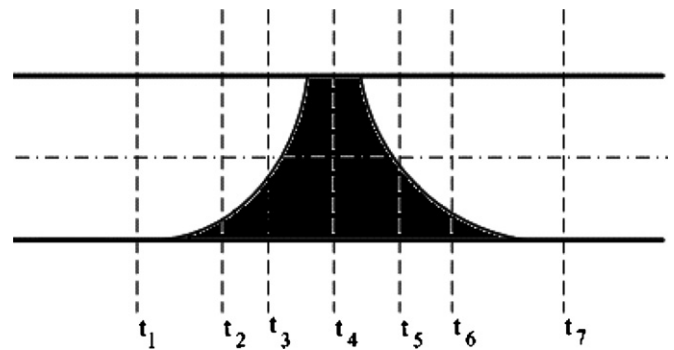
4.3. Static tests

Static tests were carried out. Figure 7 shows a twin-plane dual-modality electrical tomography (ECT/ERT) system developed by Tianjin University.

The twin-plane sensor is designed for cross-correlation velocity measurement [27, 28]. To facilitate visual observations of the flow regime, the horizontal test section (0.6 m long) is a Perspex pipe (85 mm in diameter). The material used to stimulate each flow regime is nylon plastic pellets.

The conductivity and permittivity distributions in the same plane can be obtained at the same time. The specifications of the system are given in table 3. In this paper, the identification method of two-phase flow regimes based on SVM and ECT is studied; only the outputs of ECT sensors are used.

Because of the limit in the experiment equipment size, three stratified flow samples, two annular flow samples, two

**Figure 8.** Flow regimes at different times in the test pipe.

core flow samples, two bubbly flow samples, one empty-pipe flow sample and one full-pipe flow sample were selected to test the SVM method. The results are given in table 4 and the correct identification rate is 100%, which means that the SVM method is an effective tool for flow regime identification even though there are fewer training samples.

A half volume of the test pipe was filled with nylon plastic pellets and the two ends of the test pipe were sealed up. The test pipe was first inclined from 0° to 180° and then from 180° to 0°. The flow regime as shown in figure 8 was obtained at different times $t_i, i = 1, 2, \dots, 7$. The identification results are given in table 5. The flow regimes at different times can be identified online correctly.

4.4. Dynamic experiments

The oil–gas two-phase flow experiment in a horizontal pipe was carried out in a multiphase flow loop at Tianjin University. The system and the measuring section of the flow loop facility are shown in figure 9, and the inner diameter is 85 mm. The left and right sensor planes in figure 9 are called plane 1 and plane 2, respectively.



Figure 9. System and the measuring section of the flow loop.

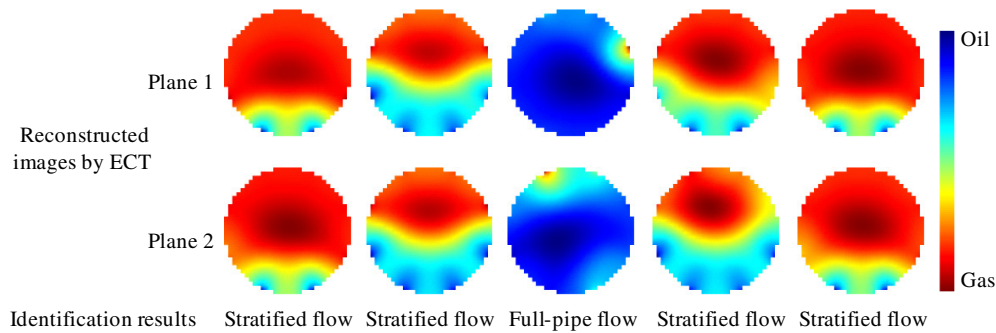


Figure 10. Dynamic identification results.

Table 4. Identification results for static experiments.

Flow regime	Empty-pipe	Core	Annular	Stratified	Bubbly	Full-pipe
Total	1	2	2	3	2	1
Correct	1	2	2	3	2	1
Identification rate	100%	100%	100%	100%	100%	100%

Table 5. Identification results at different times.

Time	Flow regime	Identification result
t_1	Empty-pipe flow	Empty-pipe flow
t_2	Stratified flow	Stratified flow
t_3	Stratified flow	Stratified flow
t_4	Full-pipe flow	Full-pipe flow
t_5	Stratified flow	Stratified flow
t_6	Stratified flow	Stratified flow
t_7	Empty-pipe flow	Empty-pipe flow

Flow regime identification results are compared with reconstructed images in figure 10. The identification results are correct.

5. Conclusions

The SVM method can identify the flow regime of oil-gas two-phase flows. Using the PCA method, the dimension of

the inputs (capacitance measurements) is decreased from 66 to 14. A DDAG for multi-class classification is presented. Simulation and experiments were carried out, indicating that the presented method is feasible. With a small number of training sets, the SVM has good generalization ability. It provides a new method to identify the flow regime for the multi-phase flow. For each flow regime, this method can be used to discriminate different void fractions between 0 and 100% given more training sets. Take stratified flow as an example: stratified (1/4), stratified (1/2), stratified (2/3) and stratified (3/4) flows corresponding to different void fractions can be studied if needed.

Acknowledgments

The authors would like to thank the National Natural Science Foundation of China (60532020, 60820106002, 60672076) and the High Technique Researching and Developing Project

of China (2006BAI03A00). The authors would also like to thank Professor Wuqiang Yang at the University of Manchester for revising this manuscript.

References

- [1] Rouhani S Z and Sohal M S 1983 Two-phase flow patterns: a review of research results *Prog. Nucl. Energy* **11** 219–59
- [2] Hassan A R and Kabir C S 1992 Two-phase flow in vertical and inclined annuli *Int. J. Multiphase Flow* **18** 279–93
- [3] Warsito W and Fan L S 2001 Measurement of real-time flow structures in gas–liquid and gas–liquid–solid flow systems using electrical capacitance tomography (ECT) *Chem. Eng. Sci.* **56** 6455–62
- [4] Dyakowski T 1996 Process tomography applied to multi-phase flow measurement *Meas. Sci. Technol.* **7** 343–53
- [5] Schleicher E, da Silva M J, Thiele S, Li A, Wollrab E and Hampel U 2008 Design of an optical tomograph for the investigation of single- and two-phase pipe flows *Meas. Sci. Technol.* **19** 094006
- [6] Liu S, Yang W Q, Wang H, Jiang F and Su Y 2001 Investigation of square fluidized beds using capacitance tomography: preliminary results *Meas. Sci. Technol.* **12** 1120–5
- [7] Ismail I, Gamio J C, Bukhari S F A and Yang W Q 2005 Tomography for multi-phase flow measurement in the oil industry *Flow Meas. Instrum.* **16** 145–55
- [8] Isaksen Ø 1996 A review of reconstruction techniques for capacitance tomography *Meas. Sci. Technol.* **7** 325–37
- [9] Yang W Q and Peng L H 2003 Image reconstruction algorithms for electrical capacitance tomography *Meas. Sci. Technol.* **14** R1–13
- [10] Xie C G, Huang S M, Holy B S, Thorn R, Lenn C, Snowden D and Beck M S 1992 Electrical capacitance tomography for flow imaging: system model for development of image reconstruction algorithms and design of primary sensors *IEE Proc. G* **139** 89–98
- [11] Dong F, Liu X P, Deng X, Xu L J and Xu L A 2001 Identification of two-phase flow regimes in horizontal, inclined and vertical pipes *Meas. Sci. Technol.* **12** 1069–75
- [12] Jeanmeure L F C, Dyakowski T, Zimmerman W B J and Clark W 2002 Direct flow-pattern identification using electrical capacitance tomography *Exp. Therm. Fluid Sci.* **26** 763–73
- [13] Warsito W and Fan L-S 2001 Neural network based multi-criterion optimization image reconstruction technique for imaging two- and three-phase flow systems using electrical capacitance tomography *Meas. Sci. Technol.* **12** 2198–210
- [14] Marashdeh Q, Warsito W, Fan L-S and Teixeira F L 2006 A nonlinear image reconstruction technique for ECT using a combined neural network approach *Meas. Sci. Technol.* **17** 2097–103
- [15] Ortiz-Alemán C and Martin R 2005 Two-phase oil–gas flow imaging by simulated annealing *J. Geophys. Eng.* **2** 32–7
- [16] Ortiz-Alemán C and Martin R 2005 Inversion of electrical capacitance tomography data by simulated annealing: application to real two-phase gas–oil flow imaging *Flow Meas. Instrum.* **16** 157–62
- [17] Mohamad-Saleh and Hoyle B S 2002 Determination of multi-component flow process parameters based on electrical capacitance tomography data using artificial neural networks *Meas. Sci. Technol.* **13** 1815–21
- [18] Xie D L, Ji H F, Huang Z Y and Li H Q 2004 An online flow pattern identification system for gas–oil two-phase flow using electrical capacitance tomography *Conf. IMTC 2004—Instrumentation and Measurement Technology (Como)* pp 2320–5
- [19] Yan H, Liu Y H and Liu C T 2004 Identification of flow regimes using back-propagation networks trained on simulated data based on a capacitance tomography sensor *Meas. Sci. Technol.* **15** 432–6
- [20] Vapnik V 1998 *Statistical Learning Theory* (New York: Wiley)
- [21] Dong J X, Krzyzak A and Suen C Y 2005 An improved handwritten Chinese character recognition system using support vector machine *Pattern Recogn. Lett.* **26** 1849–56
- [22] Tan C, Dong F and Wu M M 2007 Identification of gas/liquid two-phase flow regime through ERT-based measurement and feature extraction *Flow Meas. Instrum.* **18** 255–61
- [23] Platt J, Cristianini N and Taylor N 2000 Large margin DAG's for multiclass classification *Advances in Neural Information Processing Systems* (Cambridge, MA: MIT Press) pp 547–53
- [24] Li J and Zhang Y 2006 Interactive sensor network data retrieval and management using principal components analysis transform *Smart Mater. Struct.* **15** 1747–57
- [25] Deibele J M, Luepschen H and Leonhardt S 2008 Dynamic separation of pulmonary and cardiac changes in electrical impedance tomography *Physiol. Meas.* **29** S1–14
- [26] Kerschen G, De Boe P, Golinval J-C and Worden K 2005 Sensor validation using principal component analysis *Smart Mater. Struct.* **14** 36–42
- [27] Deng X, Dong F, Xu L J, Liu X P and Xu L A 2001 The design of a dual-plane ERT system for cross correlation measurement of bubbly gas/liquid pipe flow *Meas. Sci. Technol.* **12** 1024–31
- [28] Lucas G P and Jin N D 2001 Measurement of the homogeneous velocity of inclined oil-in-water flows using a resistance cross correlation flow meter *Meas. Sci. Technol.* **12** 1529–37